JCB Article

A requirement for cytoplasmic dynein and dynactin in intermediate filament network assembly and organization

Brian T. Helfand,[1] Atsushi Mikami,[2] Richard B. Vallee,[2] and Robert D. Goldman[1]

[1]Northwestern University School of Medicine, Department of Cell and Molecular Biology, Chicago, IL 60611
[2]Columbia University, Department of Pathology, Division of Cell and Molecular Biology, New York, NY 10032

We present evidence that vimentin intermediate filament (IF) motility in vivo is associated with cytoplasmic dynein. Immunofluorescence reveals that subunits of dynein and dynactin are associated with all structural forms of vimentin in baby hamster kidney-21 cells. This relationship is also supported by the presence of numerous components of dynein and dynactin in IF-enriched cytoskeletal preparations. Overexpression of dynamitin biases IF motility toward the cell surface, leading to a perinuclear clearance of IFs and their redistribution to the cell surface. IF-enriched cytoskeletal preparations from dynamitin-overexpressing cells contain decreased amounts of dynein, actin-related protein-1, and p150^{Glued} relative to controls. In contrast, the amount of dynamitin is unaltered in these preparations, indicating that it is involved in linking vimentin cargo to dynactin. The results demonstrate that dynein and dynactin are required for the normal organization of vimentin IF networks in vivo. These results together with those of previous studies also suggest that a balance among the microtubule (MT) minus and plus end–directed motors, cytoplasmic dynein, and kinesin are required for the assembly and maintenance of type III IF networks in interphase cells. Furthermore, these motors are to a large extent responsible for the long recognized relationships between vimentin IFs and MTs.

Introduction

Intermediate filaments (IFs),* well known for their role as major cytoskeletal elements, are also remarkably dynamic with respect to their assembly properties and organization (Prahlad et al., 1998; Yoon et al., 1998). One of the most interesting of these dynamic properties relates to IF motility, which is most obvious during the early stages of fibroblast cell spreading. During cell spreading, nonfilamentous nonmembrane-bound vimentin aggregates, termed particles, are observed to move bidirectionally at high rates of speed ($\sim$1 μm/s). These particles appear to be converted into short motile IFs or squiggles, which are incorporated into the longer vimentin fibrils that typify the interphase IF networks of fibroblasts (Prahlad et al., 1998). These fibrils also move bidirectionally (Yoon et al., 1998; Roy et al., 2000; Wang et al., 2000). The movements of the various forms of vimentin are to a great extent dependent on microtubules (MTs) as demonstrated by their sensitivity to inhibitors such as nocodazole (Prahlad et al., 1998; Yoon et al., 1998). In vitro evidence for the role of MTs in IF movements comes from studies of squid axoplasm and bovine spinal cord extracts (Prahlad et al., 2000; Shah et al., 2000). These studies have provided more direct evidence that the various forms of IF protein, including particles and short IFs, are transported rapidly along single MTs in a bidirectional fashion. Together, these observations suggest that both plus and minus end–directed MT-associated motor proteins may be responsible for many of the motile properties of IFs (Chou et al., 2001).

Conventional kinesin and cytoplasmic dynein are the major MT plus end–directed (anterograde) and minus end–directed (retrograde) motors, respectively. To date, all studies on IF motility in vivo have focused on the interactions between IFs and kinesin (Gyoeva and Gelfand, 1991; Prahlad et al., 1998, Kreitzer et al., 1999; Yabe et al., 1999). The results of these studies show that extended vimentin IF networks retract toward the nucleus, following either the microinjection of kinesin antibodies (Gyoeva and Gelfand, 1991; Prahlad et al., 1998) or the expression of a mutant kinesin dynein

Address correspondence to Robert D. Goldman, Dept. of Cell and Molecular Biology, Northwestern University School of Medicine, Ward Building #11-145, 303 East Chicago Ave., Chicago, IL 60611. Tel.: (312) 503-4215. Fax: (312) 503-0954. E-mail: r-goldman@northwestern.edu

*Abbreviations used in this paper: Arp1, actin-related protein-1; GFP, green fluorescent protein; HC, dynein heavy chain; IC, dynein intermediate chain; IF, intermediate filament; LC, light chain; LIC, dynein light intermediate chain; MT, microtubule; NF, neurofilament.

Key words: intermediate filaments; vimentin; dynein; dynactin; cytoskeleton

heavy chain (HC) (Navone et al., 1992). Therefore, the activity of kinesin is required for the maintenance of extended vimentin IF networks in vivo. It has also been shown that kinesin is associated with the rapidly moving vimentin particles in spreading cells and that this association is required for the assembly of IF networks in spread cells (Prahlad et al., 1998). Similarly, kinesin and neurofilament (NF) interactions have been reported in neurons (Yabe et al., 1999). Other studies have demonstrated that IF proteins can interact with kinesin in vitro (Liao and Gundersen, 1998; Yabe et al., 1999; Prahlad et al., 2000). In particular, it appears that the tail portion of the kinesin HC and a 62-kD kinesin light chain (LC) directly bind to vimentin in vitro (Avsyuk et al., 1995).

As indicated above, the movements of the various forms of IFs are bidirectional, suggesting that the minus end–directed MT-based motor cytoplasmic dynein, may also be involved in regulating the motility, assembly, and organization of IFs. All of the evidence in favor of this possibility comes from in vitro observations of bovine spinal cord extracts showing that polymerized NFs move toward the minus ends of MTs in association with dynein (Shah et al., 2000). This was demonstrated by the addition of dynein antibodies to preparations of fluorescent-labeled native NFs containing brain MTs, which decreased minus end–directed NF motility. Preparations of native NFs also contained components of dynein and dynactin as shown by immunoblotting. However, there is currently no evidence demonstrating that dynein is responsible for the retrograde motility and the normal assembly and maintenance of IF networks in vivo.

Cytoplasmic dynein is a large complex containing HC, dynein intermediate chain (IC), dynein light intermediate chain (LIC), and LC subunits (Vallee and Sheetz, 1996). The HCs contain the motor domain responsible for interacting with and translocating along MTs. The other subunits have been implicated in cargo binding and targeting (Karki and Holzbaur, 1995; Vaughan and Vallee, 1995; Echeverri et al., 1996; Purohit et al., 1999; Tai et al., 1999; Tynan et al., 2000b; Yano et al., 2001). Dynactin is a dynein-associated complex that contains ~11 different subunits required for most, if not all, dynein-mediated activities. This complex has been implicated in linking dynein to mitotic kinetochores (Echeverri et al., 1996) and membranous organelles (Burkhardt et al., 1997; Roghi and Allan, 1999). It has also been reported to stimulate dynein processivity along MTs in vitro (King and Schroer, 2000). An important approach to determining dynein function in vivo has involved the overexpression of the 50-kD dynamitin subunit of dynactin. This dissociates the dynactin complex, thereby disrupting dynein function without affecting kinesin (Echeverri et al., 1996; Burkhardt et al., 1997). Increasing the level of dynamitin in cells has helped to reveal the importance of cytoplasmic dynein in mitosis (Echeverri et al., 1996; Sharp et al., 2000; Howell et al., 2001) in the intracellular distribution of membrane-bound organelles, such as the Golgi apparatus and lysosomes (Burkhardt et al., 1997; Presley et al., 1997), in the transport of virus particles to the nucleus (Suomalainen et al., 1999) and in centrosome assembly (Young et al., 2000).

A full understanding of the mechanisms underlying the motility of vimentin requires the identification of the motor(s) responsible for retrograde movements. To this end, we have performed experiments aimed at determining whether the various forms of IF protein are associated with cytoplasmic dynein and dynactin. We have also determined whether the disruption of dynein function alters the motility and organization of vimentin. Furthermore, we have initiated studies to determine whether dynein and dynactin are associated with vimentin IFs in vitro. Our data indicate that vimentin is a major cargo for cytoplasmic dynein in fibroblasts. These results, together with previous studies on kinesin, suggest that the motility and organization of IF networks are dependent on a balance of MT-associated minus end– and plus end–directed motors.

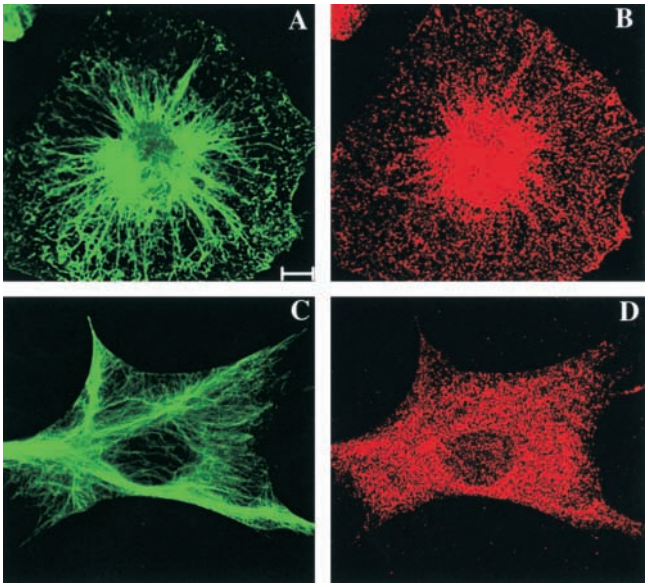

Figure 1. **Vimentin, dynein, and dynactin in spreading and spread fibroblasts.** Approximately 45 min after trypsinization and replating, BHK-21 cells were processed for immunofluorescence with antibodies directed against vimentin and HC. At low magnification, the overall staining pattern of HC was similar to vimentin throughout the early stages of cell spreading (A and B). However, ~4–6 h after replating the punctate HC staining patterns appeared randomly distributed throughout most of the cytoplasm (D). At these time points, the similarities between the staining patterns of HC and vimentin were no longer apparent (C and D) with the exception of some regions at the cell periphery (see Fig 2). (vimentin, green; HC, red). Bar, 10 μm.

Results

Relationships among IFs, dynein, dynactin, and MTs

To begin to determine whether dynein and dynactin are associated with the various forms of vimentin IFs present in baby hamster kidney (BHK-21) cells, we performed immunofluorescence studies using antibodies against vimentin and specific components of dynein and dynactin. The latter included antibodies directed against cytoplasmic LIC1 and 2, LIC2 alone, IC, HC, and the p150^{Glued} and dynamitin subunits of dynactin. In the majority of spread cells, the antibodies against dynein and dynactin revealed punctate structures throughout the entire cytoplasm (Fig. 1 D). Double labeling with vimentin antibody showed no general association of either dynein or dynactin with the extensive IF net-

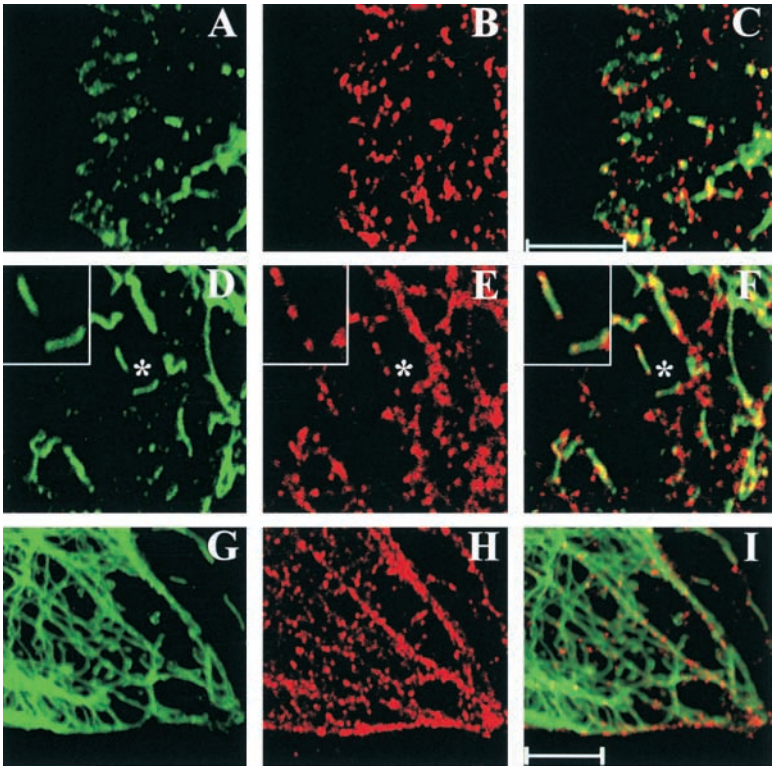

Figure 2. **Different structural forms of vimentin associate with dynein and dynactin.** Spreading cells were processed for immunofluorescence at 45–90 min after replating. At low magnification, these cells appeared as in Fig. 1, A and B. At higher magnification, it became obvious that many vimentin particles and squiggles were associated with dynein and dynactin (A–F). In some cases, dynein and dynactin were located at one or both ends of vimentin squiggles (D–F, insets). In the peripheral regions of some extensively spread cells fixed at ~4–6 h after replating, longer vimentin fibrils were also associated with dynein and dynactin (G–I). Asterisks denote area shown in insets. (A, D, and G, vimentin [green]; B, E, and H, HC [red]; C, F, and I are overlays in which colocalization is shown in yellow). Bars, 5 μm.

work (Fig. 1, C and D). However, in the peripheral regions of the most extensively flattened cells (62/550), an association between the IF and the dynein/dynactin staining patterns could be discerned (Fig. 2, G–I).

To visualize the various forms of vimentin, BHK-21 cells were fixed for double label immunofluorescence at different times during the spreading process (Prahlad et al., 1998). At early stages, the overall patterns of dynein, dynactin, and vimentin appeared similar. In the case of the HC antibody, for example, the majority of cells (178/200) observed at 45 min displayed such similarities (Fig. 1, A and B). This association was maintained for 2–4 h or until the cells were fully spread. More detailed observations of the different forms of vimentin in cells at 45 min after replating showed that ~65% (523/800) of the vimentin particles were closely associated with dynein and dynactin (Fig. 2, A–C). Within 1.5 h after replating, there were fewer vimentin particles, but numerous squiggles were present in the peripheral cytoplasm (Prahlad et al., 1998). The majority of vimentin squiggles (~85% [424/500]) were also associated with dynein and dynactin (Fig. 2, D–F). Interestingly, spots of dynein and dynactin frequently appeared at one or both ends of squiggles (Fig. 2, D–F, in-

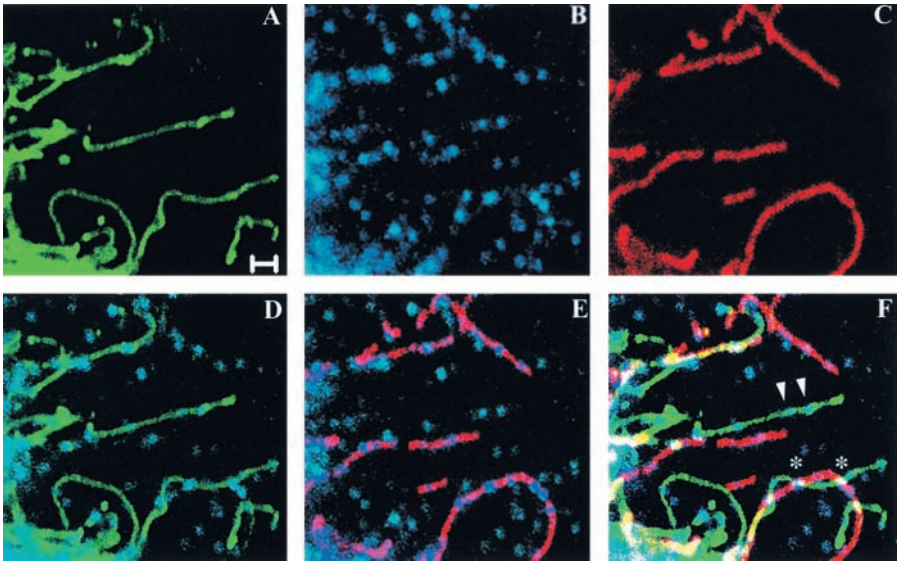

Figure 3. **Intermediate filaments associate with dynein, dynactin, and microtubules.** To determine the relationships among vimentin, MTs, dynein, and dynactin in situ, spread BHK-21 cells were processed for triple label immunofluorescence using antivimentin (A), HC (B), and tubulin (C). The different structural forms of vimentin (A) were most obvious in thinly spread regions of the cell periphery. Dynein appeared as punctate structures throughout the cytoplasm (B). Overlays of vimentin and HC (D) showed that particles, squiggles, and longer fibrils were associated with dynein. Dynein was present at many of the intersections between vimentin and MTs (F, asterisks). In some cases, dynein appeared to be associated with vimentin structures that were not associated with MTs (E; see arrowheads in F). (A, D, and F, vimentin [green]; B, D, E, and F, HC [blue]; C, E, and F, MTs [red]. F is an overlay of A, B, and C in which colocalization between vimentin and dynein appears as blue green, vimentin and MTs as yellow, HC and MTs as lavender, and vimentin, HC, and MTs as white). Bar, 2 μm.

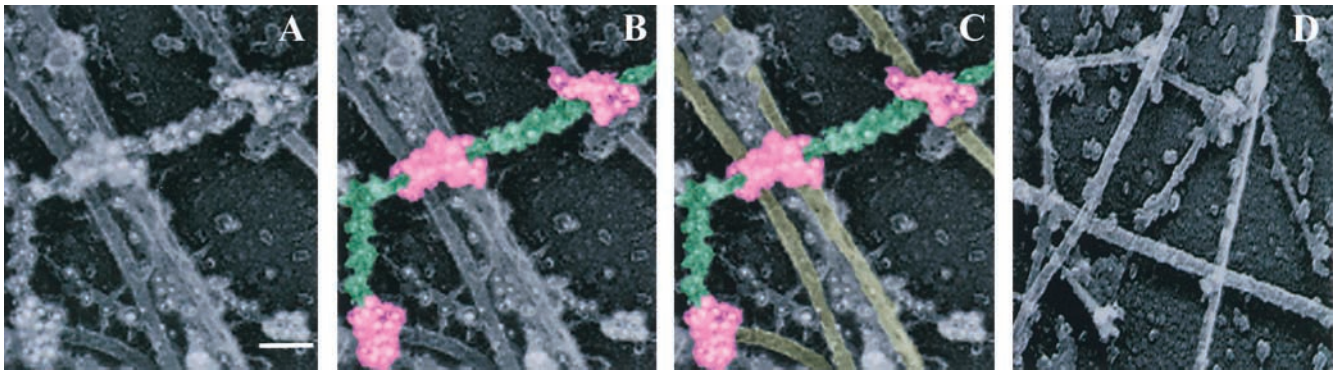

Figure 4. **Ultrastructural observations.** BHK-21 cells were processed for platinum replica EM using a technique that preserves IFs and MTs (Svitkina et al., 1995). Although there was an ~5-nm increase in thickness due to the platinum and carbon coatings, the ratio between the diameter of IFs and MTs in these preparations was ~1:2.5, which is consistent with the known ratio of the diameters of IFs (10 nm) to MTs (25 nm). Antibodies conjugated with 10 and 18 nm gold particles were used to visualize vimentin and HC, respectively (A–C). Dynein was often found at intersections between vimentin and MTs (A–C), consistent with the light microscope studies (see Fig. 3). In B and C, arrays of 10 nm gold particles along vimentin IFs are colored green, and clusters of 18 nm gold particles representing dynein are seen in pink. In C, MTs are colored yellow. Controls for these experiments are shown in D (secondary antibodies only; as described in Materials and methods). Bar, 100 nm.

sets). After 4 h, the associations among vimentin, dynein, and dynactin were once again limited to the peripheral regions of cells (see above) where dynein and dynactin usually showed a punctate distribution along the longer IFs (Fig. 2, G–I).

We also determined the relationships among particles, squiggles, longer IFs, dynein, and MTs in spread cells using triple label immunofluorescence (Fig. 3, A–C). To this end, we made counts of the spots stained with the HC antibody in randomly selected peripheral regions of 10 spread cells (Fig. 3 B). We determined that 48% (480/1,000) of these spots were associated with vimentin (Fig. 3, A and B, and D, overlay). Of these spots, ~21% (214/1,000) were located at apparent intersections between vimentin and MTs (Fig. 3 F, asterisks). The other 27% (266/1,000) of the spots colocalized with vimentin not associated with MTs (Fig. 3 F, arrowheads). In addition, some dynein (~10% [103/1,000]) appeared to be associated with MTs but not vimentin (Fig. 3, D compared with E). Other dynein-positive spots did not appear to be associated with either vimentin or MTs (~42% [417/1,000]) (Fig. 3, B and F).

We also studied the association among vimentin, dynein, dynactin, and MTs at the ultrastructural level. Platinum replica double immunogold electron microscopic preparations confirmed the immunofluorescence observations (Fig. 4, A–C compared with Fig. 3, A–F). For example, dynein was present in regions of close association between vimentin IFs and MTs (Fig. 4, A–C). Controls for these preparations are depicted in Fig. 4 D (see Materials and methods).

Further evidence in support of an association among IFs, dynein, and dynactin

We initiated studies to analyze the nature of the interactions among dynein, dynactin, and vimentin. To this end, various cell extraction procedures (see Materials and methods) were used to determine whether the association among vimentin IFs, dynein, and dynactin was retained compared with unextracted fixed cells (Fig. 5, A–D). Similar procedures have been used to document the associations between dynactin and different cytoskeletal components (Garces et al., 1999). For this purpose, different concentrations of detergents and salt were used. Varying the salt concentration between 0.1 and 1.0 M did not appear to alter the percentage of cells showing similar patterns among vimentin, dynein, and dy-

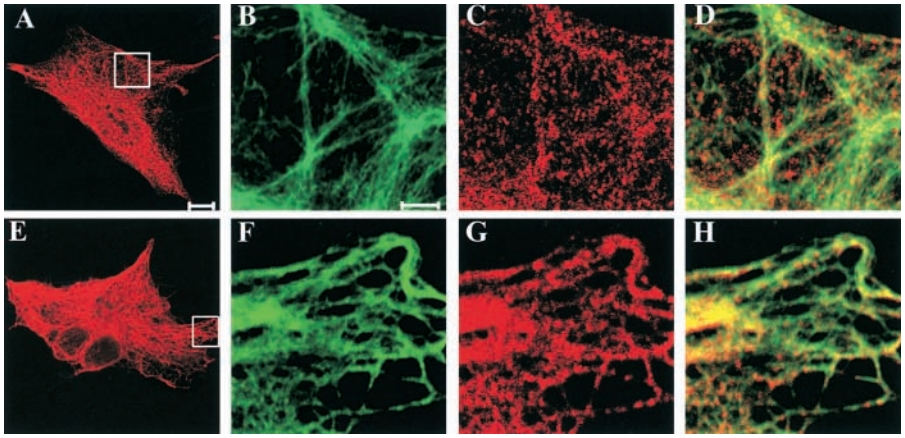

Figure 5. **The association between dynein, dynactin, and vimentin is retained after detergent extraction.** In the peripheral regions of some unextracted formaldehyde-fixed BHK-21 cells, an association among vimentin (B), dynein, and dynactin (A) was apparent (also see Fig. 2). However, after the preparation of IF-enriched cytoskeletons, which removes most membranous organelles (C compared with G), the majority of cells showed an obvious association among dynein, dynactin, and vimentin (E–H). Identical associations were observed with all of the dynein and dynactin antibodies. (A, C, E, and G, HC [red]; B and F, vimentin [green]; D and H are overlays in which colocalization is shown in yellow). Bars: (A and E) 10 μm; (B–D and F–H) 5 μm.

Table I. **The percentage of cells displaying similar immunofluorescence patterns after incubation with various extraction buffers and staining with vimentin and dynein antibodies**

	No NaCl added			No NaCl added			1 M NaCl		
	Average	SD	N	Average	SD	N	Average	SD	N
	%			%			%		
Digitonin									
0.1%	16	±3	147	16	±7	200	11	±4	183
0.5%	24	±11	129	22	±11	100	13	±6	160
1.0%	34	±15	151	32	±1	100	12	±3	186
NP-40									
0.1%	43	±10	200	31	±15	150	41	±1	150
0.5%	67	±16	100	80	±12	175	74	±20	300
1.0%	73	±9	113	62	±3	100	83	±9	130
Triton X-100									
0.1%	59	±12	180	37	±4	200	46	±8	220
0.5%	64	±6	134	88	±6	200	92	±3	100
1.0%	90	±11	100	66	±1	180	81	±18	100
IF prep				98	±1	250			

To determine the extent of association among vimentin, dynein, and dynactin, BHK-21 cells were incubated with various extraction solutions before fixation. All extraction solutions contained 100 mM Hepes, pH 7.4, 60 mM Pipes, and protease inhibitors (see Materials and methods). In addition, solutions contained either 0.1, 0.5, or 1.0% digitonin, NP-40, or Triton X-100 and either 0.5 M,1 M, or no NaCl. The "IF prep" extraction buffer contained 1% Triton X-100, 1 mg/ml DNase 1, and 0.5 M NaCl (see Materials and methods). In all cases, data was pooled from three different experiments for each detergent and each salt concentration. The average percentage of cells displaying similar patterns between vimentin and dynein HC are represented in the table.

nactin by immunofluorescence (Table I). However, the percentage of cells showing this association did vary based on the concentration but not the type of detergent used in the extraction buffer. After 0.1–0.5% detergent extraction, there were slight increases in the number of cells showing similar patterns of vimentin, dynein, and dynactin (Table I). When 1.0% detergent was used, the association became obvious in 79% of the cells (Table I). Standard IF-enriched cytoskeletons using 1.0% Triton X-100 (see Materials and methods) showed a close association between dynein and dynactin in all regions of the vast majority of cells (~98% [195/200]) (Fig. 5, E–H, and Table I). Ultrastructural analysis of these preparations confirmed the immunofluorescence results showing that dynein localized along individual vimentin IFs (unpublished data). Analysis of the protein content of IF-enriched cytoskeletal preparations by SDS-PAGE and immunoblotting revealed, in addition to vimentin, the presence of components of dynein and dynactin including LIC2, LIC1 and 2, IC, HC, dynamitin, p150^{Glued}, and actin-related protein-1 (Arp1) (Fig. 6).

Disruption of dynactin in vivo alters the organization of vimentin IFs

The morphological and biochemical relationships described above suggest that dynein and dynactin are involved in regulating both the motility and maintenance of the organization of vimentin IFs. Dynamitin overexpression might therefore be expected to affect the organization of the vimentin IF network. To test this possibility, BHK-21 cells were transfected with myc-dynamitin cDNA (see Materials and methods), which has been shown to uncouple the dynactin complex and disrupt dynein function (Echeverri et al., 1996). Coverslips containing dynamitin-expressing BHK-21 cells were fixed and stained with myc and vimentin antibodies at 6, 12, and 48 h after transfection. Other coverslips were processed for double label immunofluorescence using antibodies directed against vimentin and either the 58K Golgi protein, tubulin, or phalloidin. In these cases, parallel cultures on coverslips were fixed and stained with only myc antibodies to determine the number of transfected cells, which was always ≥90%.

In ~90% of nontransfected cells, the vimentin network extended from the nucleus to the cell periphery with the majority of vimentin IFs concentrated in the perinuclear region

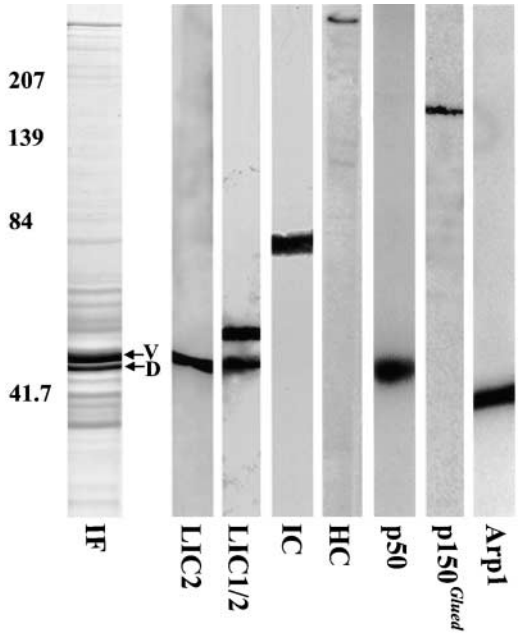

Figure 6. **IF-enriched cytoskeletal preparations of BHK-21 cells were prepared and analyzed by SDS-PAGE and immunoblotting.** Lane IF is a Coomassie stain showing that vimentin (V) and desmin (D) are the major proteins present in IF-enriched cytoskeletal preparations. Immunoblot analysis of these same preparations shows that many of the components of the dynein and dynactin complexes are present; LIC2, LIC1 and 2, IC, HC, dynamitin (p50), p150^{Glued}, and Arp1.

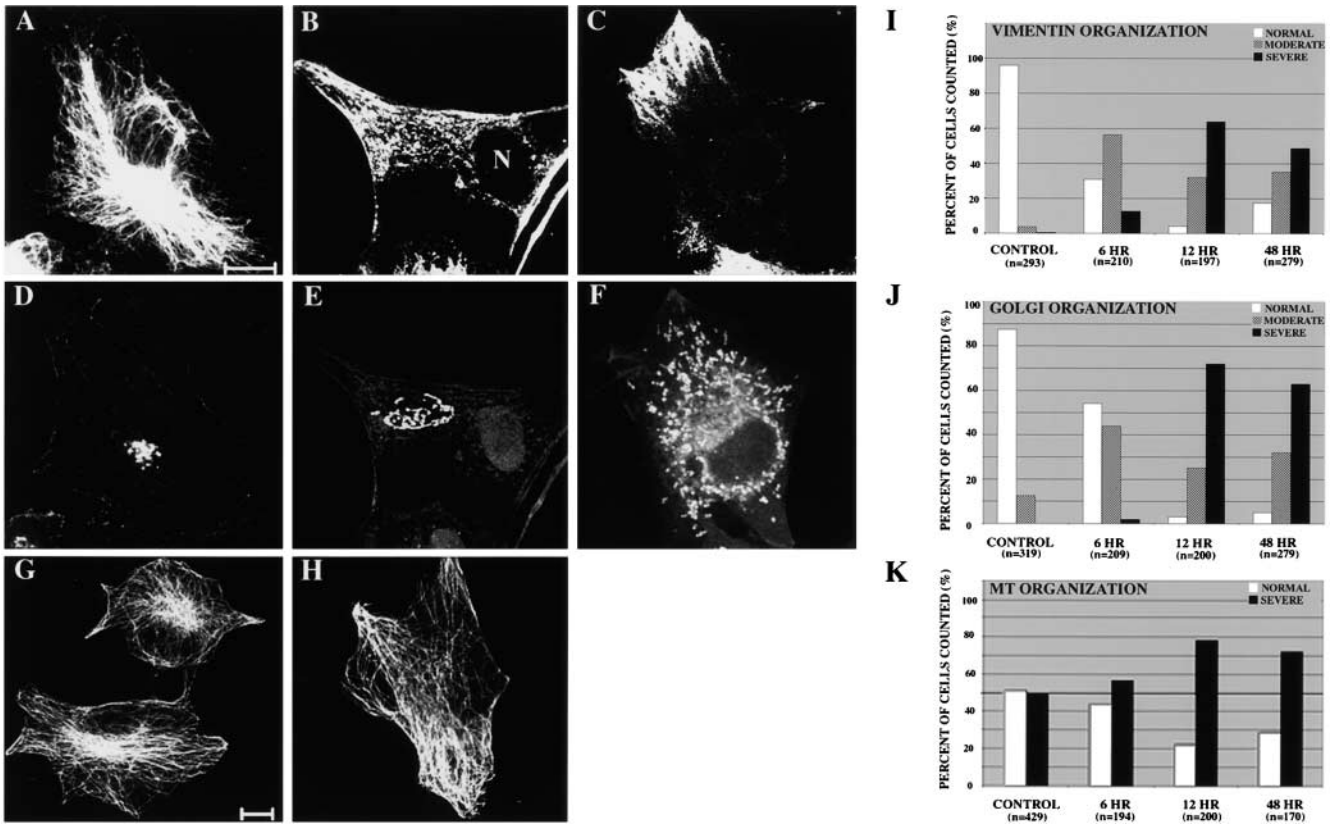

Figure 7. **Dynamitin overexpression induces alterations in the organization of the vimentin IF.** BHK-21 cells were transfected with myc-dynamitin cDNA and fixed at 6, 12, and 48 h after transfection. Controls for each time point involved staining separate coverslips with c-myc antibody (unpublished data). Cells in A–F were double labeled with vimentin (A–C) and the 58K Golgi protein (D–F) antibodies. MTs are depicted in G and H. A variety of phenotypes were observed at each time point. Therefore, the percentage of cells showing different vimentin, Golgi, and MT phenotypes was determined for each time point (I–K). The number of cells exhibiting a "normal" vimentin or Golgi network, such as those seen in (A and D), decreased with time after dynamitin transfection (I and J). The number of cells showing a "moderate" vimentin or Golgi phenotype (B and E) or a "severe" vimentin or Golgi phenotype (C and F) increased over time post transfection (I and J). Similarly, there was a decrease in the number of cells displaying a "normal" MT network (G and K). Dynamitin overexpression induced a dispersal of MTs from the MTOC ("severe" phenotype; H and K). The dispersion of MTs was not observed until after the vimentin and Golgi phenotypes became apparent (compare I, J, and K). N, nucleus. Bars, 10 μm.

("normal" phenotype) (Fig. 7, A and I). Within 6 h after transfection, >70% of cells that were myc positive showed an obvious reduction of vimentin IFs in the perinuclear region. However, numerous vimentin particles and squiggles were still seen throughout the cytoplasm ("moderate" phenotype) (Fig. 7, B and I). After 12 h, ~64% of the overexpressing cells contained barely detectable levels of vimentin staining in the perinuclear region with intense staining near the cell surface ("severe" phenotype) (Fig. 7, C and I). These overexpressing cells appeared similar to those fixed at later times up to 48 h after transfection. In all cells containing the severe phenotype, some vimentin particles remained evident in the region between the nucleus and the cell surface (Fig. 7 C and Fig. 8, A, D, and G). As a control, dynamitin-overexpressing cells were plated into nocodazole for 2, 4, and 8 h. In these cells, vimentin remained concentrated in the perinuclear area and did not become dispersed to the cell periphery (unpublished data).

In ~88% of nontransfected cells, there was a well-defined perinuclear Golgi network ("normal" phenotype) (Fig. 7, D and J). As expected, the number of cells with this control phenotype decreased over time after transfection (Burkhardt et al., 1997). At ~6 h, the Golgi began to disperse from the perinuclear region as sac-like structures ("moderate" phenotype) (Fig. 7, E and J). After 12 h (Fig. 7, F and J), the components of the Golgi apparatus were fragmented and dispersed throughout the cytoplasm in ~72% of the cells. Similar results were seen in the majority of cells at 48 h after transfection ("severe" phenotype) (Fig. 7, F and J). The results of the double label experiments showed that cells with the severe vimentin phenotype also exhibited punctate Golgi staining distributed throughout the cytoplasm (Fig. 7, C and F). Interestingly, double label immunofluorescence at early time points (i.e., 6 h) revealed a vimentin phenotype before any apparent change in Golgi organization (Fig. 7, I and J).

The number of MTs focused near the MTOC also decreased as a function of time after dynamitin overexpression (Burkhardt et al., 1997; Quintyne et al., 1999). MTs were normally focused near the nucleus (MTOC) in ~50% of nontransfected cells ("normal" phenotype) (Fig. 7, G and K). After transfection with dynamitin, there was a decrease in the number of cells displaying this pattern of MTs ("severe" phenotype) (Fig. 7, H and K). Although the number of cells showing the severe phenotype increased slightly at 6 h after transfection, a significant change was not observed until 12 h (Fig. 7 K). Thus, the dynamitin-induced effects

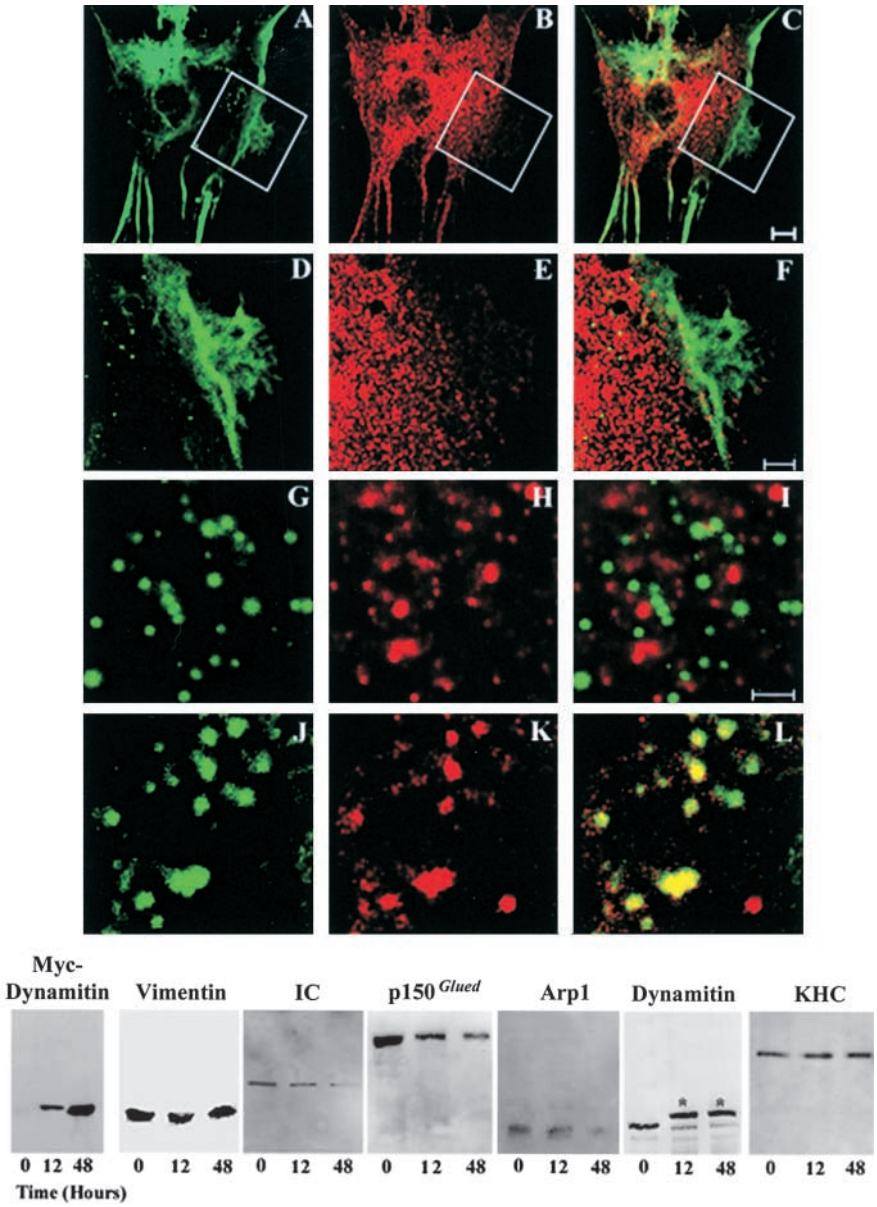

Figure 8. **Vimentin association with specific components of dynein and dynactin is decreased in cells overexpressing dynamatin.** 48 h after transfection with myc-dynamitin cDNA, BHK-21 cells were processed for double label immunofluorescence using antibodies against dynactin, dynein (for example HC [B, E, and H] and vimentin [A, D, and G]). Overlays of these images are shown in G, F, and I. In most cells, vimentin staining was concentrated near the cell surface and particles could be seen throughout the cytoplasm (A). In many regions, there was an obvious loss of the association among the peripheral accumulations of vimentin, dynein, and dynactin (seen at low magnification in A–C; D–F depict higher magnification views of squares in A–C). In addition, vimentin particles did not appear to associate with dynein or dynactin (G–I). However, vimentin particles did retain an association with kinesin as demonstrated by double labeling with antivimentin (J) and antikinesin HC (K). (A, D, G, and J, vimentin [green]; B, E, and H, HC [red]; K, kinesin HC [red]; C, F, I, and L are overlays in which colocalization is shown in yellow). Bar: (A–C) 10 μm; (D–F) 2 μm; (G–L) 1 μm. BHK-21 cells were transfected with myc-dynamitin and whole cell protein extracts, and IF-enriched cytoskeletal preparations were prepared at 0, 12, and 48 h after transfection. Immunoblots of whole cell protein preparations revealed that myc-dynamitin expression increased as a function of time after transfection (see Myc Dynamitin). The amount of vimentin present in IF-enriched cytoskeletal preparations did not appear to change in transfected cells (see Vimentin). In contrast, the amount of dynein and dynactin present in these preparations decreased as a function of time (for example, see IC, p150^{Glued}, and Arp1). In contrast, the amounts of dynamitin and conventional kinesin in these preparations appeared unchanged (see Dynamitin and KHC). Asterisks denote the top molecular weight (MW) band showing expression of myc-dynamitin versus the bottom molecular weight (MW) band showing endogenous dynamitin in nontransfected cells.

on MT organization appeared after the vimentin and Golgi networks were dispersed. Consistent with other studies, there were no detectable effects on the F-actin networks for up to 48 h in dynamitin-overexpressing cells (unpublished data; Burkhardt et al., 1997). Similar results were also obtained with mouse 3T3 cells (unpublished data).

The association among IFs, dynein, and dynactin decreases after dynamitin overexpression

We also determined whether the association among vimentin, dynein, and dynactin was disrupted by dynamitin overexpression. BHK-21 cells were processed for double label immunofluorescence using vimentin and dynein/dynactin antibodies at 48 h after transfection. Overexpressing cells were identified by the severe vimentin phenotype (Fig. 7 C). In many peripheral regions, there appeared to be a decrease in the amount of colocalization between dynein and vimentin compared with nontransfected control cells (Fig. 8, A–F). In addition, the majority (~95% [439/510]) of the vimentin particles did not appear to colocalize with dynein regardless of their location (Fig. 8, G–I). Since we have demonstrated previously that vimentin particles are associated with conventional kinesin (Prahlad et al., 1998), it was of interest to determine whether this relationship was maintained in cells overexpressing dynamitin. As seen in Fig. 8, J–K, this association was retained.

Since the majority of cells were transfected with dynamitin, it was possible to begin to determine whether there were alterations in the association among vimentin, dynein, and dynactin at the biochemical level. For this purpose, whole cell protein extracts were prepared from control cells and cells transfected for 12 and 48 h. Immunoblot analysis

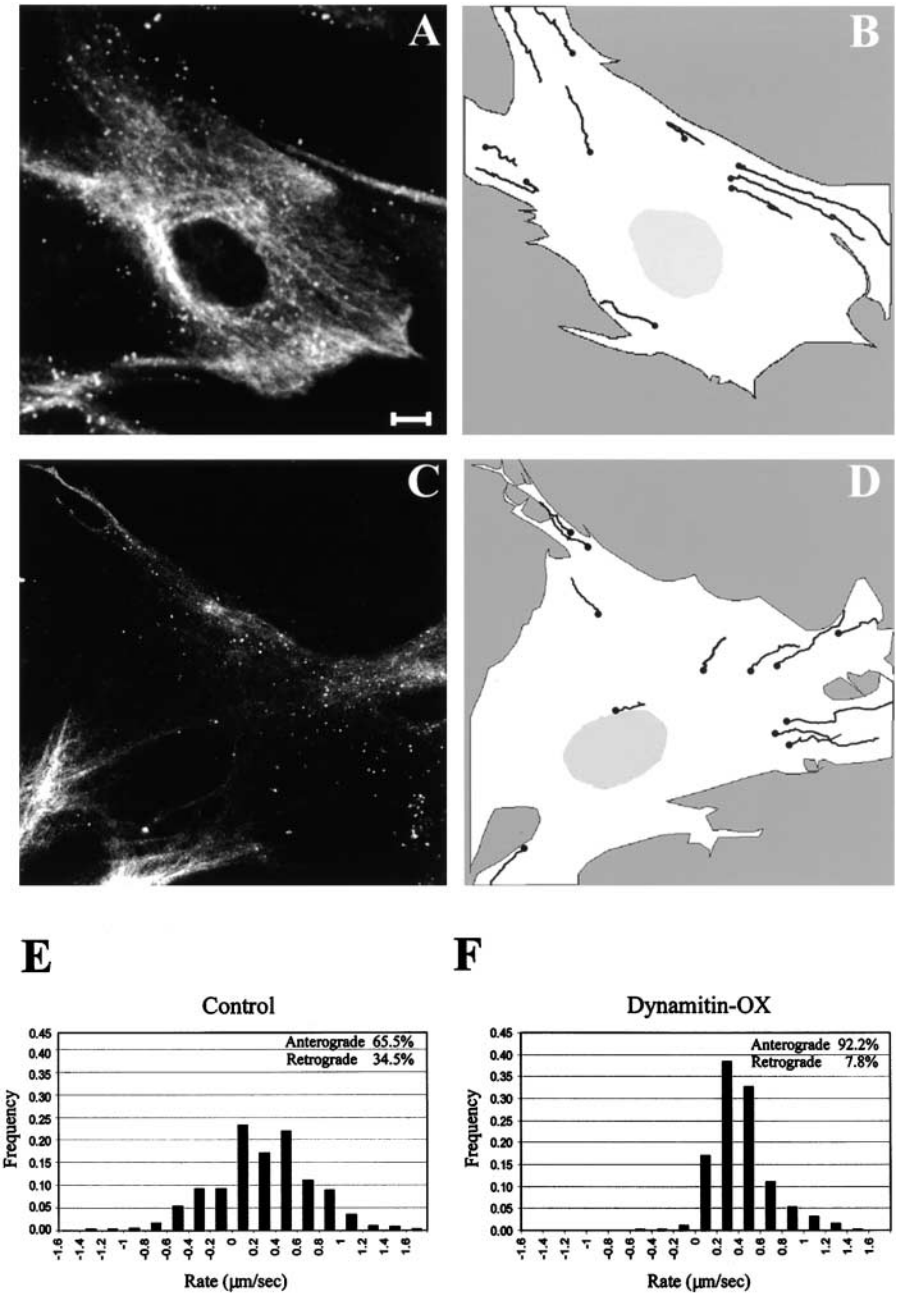

Figure 9. **Dynamitin overexpression biases GFP-vimentin particle movement towards the cell periphery.** BHK-21 cells were transfected with both GFP-vimentin and dynamitin cDNA (C). Controls were transfected with GFP-vimentin (A). The speeds and directions of particle movements were analyzed, and vector diagrams for the pathways of several examples of individual particles in a control cell and in a cell expressing dynamitin are shown (B and D). A closed circle (black) denotes the original location of vimentin particles. The solid black line indicates particle trajectories. The number of particles (frequency) that moved at a given rate is shown (E and F). Positive rates denote movements toward the periphery, and negative rates indicate movements toward the nucleus. Vimentin particles moved in the anterograde direction ~65% of the time and in a retrograde direction ~35% of the time in control cells (A and B). In contrast, dynamitin-overexpressing cells contained particles that moved in the anterograde direction ~92% of the observation time (B and D compared with E and F). Bar, 10 μm.

of these preparations revealed that the expression of myc-tagged dynamitin increased over time (Fig. 8, Myc-Dynamitin). IF-enriched cytoskeletal preparations of dynamitin-overexpressing cells were prepared at these same time points and analyzed by immunoblotting with antibodies directed against vimentin, IC, p150^{Glued}, Arp1, and dynamitin (Fig. 8). In these preparations, it appeared that the vimentin concentration did not change for periods up to 48 h after transfection (Fig. 8, Vimentin). However, there was a time-dependent decrease in the amounts of both dynein (Fig. 8, IC) and dynactin (Fig. 8, p150^{Glued} and Arp1). Identical results were obtained for the same time points with HC, LIC1 and 2, and LIC2 antibodies (unpublished data). In contrast, there was no detectable decrease in dynamitin present in these preparations (Fig. 8, Dynamitin). In addition, conventional kinesin was also retained in these preparations (Fig. 8, KHC). These results suggest that dynamitin overexpression leads to a decreased association between some but not all of the subunits of dynein/dynactin and the vimentin cargo, whereas the association of kinesin appears to be unaltered.

Disruption of the dynactin complex significantly biases the motility of vimentin

As indicated above, dynamitin overexpression induces the dispersal of the majority of vimentin toward the cell periphery, although many vimentin particles remain throughout the region between the nucleus and the cell surface. To determine the behavior of these particles, BHK-21 cells were transfected with green fluorescent protein (GFP)-vimentin cDNA. After 24 h, these same cells were transfected with either myc-dynamitin cDNA or mock transfected (see Materials and meth-

ods). 24 h after the second transfection, cells were fixed and processed for immunofluorescence using anti-myc antibodies. Because of the high dynamitin transfection rate (see above), the majority of GFP-vimentin–positive cells also expressed myc-dynamitin (unpublished data). Cells coexpressing GFP-vimentin and dynamitin exhibited phenotypes that were indistinguishable from fixed, stained BHK-21 cells transfected with only myc-dynamitin cDNA (i.e., accumulations of vimentin at the cell periphery and vimentin particles between the nuclear region and the cell surface) (Fig. 9 C).

As a control, vimentin particle movements were first analyzed in cells transfected with only GFP-vimentin. Analysis of the motility of 53 different GFP-vimentin particles selected in the peripheral regions of 12 different interphase cells was performed. The results showed that individual particles were capable of translocating bidirectionally at rates from 0.1 to ~1.7 μm/s (Fig. 9, A, B, and E). These rates are comparable to those found in spreading BHK-21 cells (Prahlad et al., 1998). Approximately 65% of vimentin particle motility was anterograde and ~35% was retrograde (Fig. 9 E). The average velocity in the anterograde direction was 0.39 ± 0.24 μm/s (n = 255 movements) (Fig. 9 E), and in the retrograde direction the rates averaged 0.43 ± 0.26 μm/s (n = 133 movements) (Fig. 9 E). Thus, GFP-vimentin particles move rapidly and in both directions in spread interphase BHK cells.

In live cotransfected cells, 51 particles from 10 different cells that exhibited a GFP-vimentin network typical of the severe phenotype were analyzed (Fig. 9 C). The results showed that particles moved anterograde ~92% of the time (n = 354 movements) (Fig. 9, D and F) with an average rate of 0.32 ± 0.23 μm/s. Therefore, the anterograde rates were not significantly different from control cells. This is also supported by the finding that kinesin remained associated with the vimentin particles (Fig. 8, J–L). In contrast, particle movements toward the nucleus occurred only ~8% of the time (n = 30 movements) (Fig. 9 F). The average retrograde rate for these particles (0.11 ± 0.05 μm/s) was significantly diminished compared with control cells (Fig. 9, E and F). Thus, dynamitin expression significantly decreased the speed and altered the directionality of vimentin particles.

Discussion

Bidirectional movements of the various forms of IFs, including particles, squiggles, and long filaments, were first described in BHK-21 cells (Prahlad et al., 1998; Yoon et al., 1998). In these cells, the anterograde movements of vimentin and the maintenance of interphase vimentin IF networks were shown to be dependent on both MTs and the plus end–directed motor kinesin (Prahlad et al., 1998). However, these and other studies have not addressed the mechanisms responsible for the retrograde components of vimentin IF motility in vivo. This study was undertaken to determine whether dynein and dynactin are also involved in the organization and maintenance of vimentin IF networks by regulating their retrograde motility in vivo.

The results of our studies show that dynein and dynactin are associated with the different forms of vimentin found in spreading cells. Similarities in the immunofluorescence patterns of vimentin, dynein, dynactin, and associations with MTs could also be seen in the peripheral regions of a small percentage of spread BHK-21 cells. These similarities were obscured throughout most of the cytoplasm due to the large number of dynein/dynactin containing membranous organelles. When membranous organelles were extracted with detergent, a more extensive association among vimentin, dynein, and dynactin components became apparent by immunofluorescence and EM. The persistence of dynein and dynactin after extraction with high concentrations of salt and detergent suggested that there was significant binding among vimentin, dynein, and dynactin. This was further supported by immunoblot analysis of IF-enriched cytoskeletal preparations, which demonstrated that each of the dynein and dynactin subunits tested were present. These blotting results also support previous studies of native NFs characterized in vitro (Shah et al., 2000).

The most dramatic result obtained in our studies was the remarkable reorganization of vimentin in cells overexpressing dynamitin. Although we expected to observe some displacement toward the cell surface, the finding that virtually all IFs were cleared from the juxtanuclear region and reorganized subjacent to the cell surface in many cells was unexpected. This result was surprising as many studies have demonstrated that virtually all perturbations of IF networks produce massive accumulations toward the cell center, usually in the perinuclear region. In the case of vimentin IFs in fibroblasts, these disruptive agents include MT inhibitors such as colchicine (Goldman, 1971), kinesin antibodies (Gyoeva and Gelfand, 1991), toxic compounds, such as acrylamide and 2,5-hexanedione (Durham et al., 1983), protein kinase A (Lamb et al., 1989), virus infection (Heath et al., 2001), and heat shock (Welch and Suhan, 1985). Since all structural forms of IFs move, the dynamitin-induced accumulation of vimentin IFs at the periphery is most likely the result of the biased motility of particles and longer IFs toward the plus ends of MTs due to the continued motor activity of kinesin. In further support of this, it was observed that vimentin particles in dynamitin-overexpressing cells are associated with kinesin and time-lapse observations demonstrate that they move in the anterograde direction 92% of the time.

It is also of interest to note that a small fraction of vimentin particles continued to move toward the nucleus in cells overexpressing dynamitin. The average rate for these movements was much slower (0.11 μm/s) than in control cells in which the average rate was calculated as 0.43 μm/s, which is consistent with cytoplasmic dynein function. Several explanations for this residual retrograde movement are possible. For example, a low level of dynein motor activity may persist in cells overexpressing dynamitin. Alternatively, this movement could be the result of an additional, yet unidentified, retrograde MT-associated motor such as an unconventional cytoplasmic kinesin (Noda et al., 2001).

The hierarchy of dynein interactions has been most extensively defined for the kinetochore (Echeverri et al., 1996; Starr et al., 1998). Dynamitin is anchored to the kinetochore through an interaction with ZW10, mutations which eliminate dynactin and dynein binding (Starr et al., 1998). In turn, dynamitin seems to serve as the principal, if not exclusive, link

to dynactin and then dynein. This conclusion is supported by the efficiency with which overexpressed dynamitin displaces the dynein and dynactin complexes from the kinetochore (Echeverri et al., 1996) and the appearance of heterologously expressed dynamitin at this site (Tai et al., 2002). Dynamitin overexpression also releases dynein from the Golgi membranes (Roghi and Allan, 1999). Whether the hierarchy of dynein interactions at the Golgi is similar to those observed at the kinetochore or mediated by a distinct mechanism involving the Arp1 backbone of the dynactin complex (Holleran et al., 1996, 2001) remains to be determined. In the current study, we find that dynamitin overexpression markedly reduces the association of both dynein and the dynactin subunits, $p150^{Glued}$ and Arp1, with vimentin. In contrast, the amount of dynamitin associated with vimentin appears to remain the same. These results are therefore consistent with the current state of understanding of the kinetochore binding hierarchy and support a general role for dynactin in dynein targeting.

It has been thought that MTs are the major factors in determining the organization of the Golgi complex and vimentin IFs, since MT depolymerizing agents induce their reorganization and distribution in cells (Goldman, 1971; Rogalski and Singer, 1984). Time-dependent observations of dynamitin-overexpressing BHK-21 cells revealed that disruptions in vimentin IFs and the Golgi complex are often evident before any changes can be observed in MT networks. In many cells observed in this study, the vimentin network appeared to become disrupted even before changes in the Golgi apparatus became apparent. Similarly, injection of NF proteins into chicken dorsal root ganglion neurons induces NF aggregation and Golgi fragmentation without altering MT organization (Straube-West et al., 1996). It has also been demonstrated that vimentin IFs directly interact with components of the Golgi apparatus (Gao and Sztul, 2001). Although a direct inhibitory effect on the motility of Golgi vesicles has been observed (Burkhardt et al., 1997; Presley et al., 1997), it is also conceivable that the effect of dynamitin on the Golgi could in part be related to the disruption of the IF network.

It is also interesting to note that all types of IFs do not appear to move in association with MT motor proteins to the same extent. For example, the microinjection of an IC antibody into epithelial cells does not obviously alter the organization of keratin IFs (Yoon et al., 2001). Similarly, dynamitin overexpression in PtK2 epithelial cells, which contain both vimentin IF and keratin IF bundles (tonofibrils), does not obviously alter the keratin IF network. However, in these same PtK2 cells dynamitin overexpression induces a peripheral redistribution of vimentin similar to that reported in this study for BHK-21 cells (unpublished data). The lack of dependence of keratin tonofibrils on MTs and their associated motor proteins is also supported by results showing that the overall organization of keratin networks appears unaltered after treatment with MT inhibitors such as colchicine or nocodazole (Osborn et al., 1980; Yoon et al., 2001). In contrast, there is evidence that a subpopulation of keratin IFs move in a fashion that appears to depend on MTs. For example, the very slow translocation of keratin tonofibrils (0.06 μm/min) and keratin squiggles (0.24 μm/min) is inhibited in the presence of nocodazole (Yoon et al., 2001). Therefore, it is possible that these types of keratin movements may be related to the functions of other MT-based motors such as unconventional kinesins (Noda et al., 2001; also see above).

In this study, we demonstrated that dynein is responsible for most of the retrograde movements of the various forms of vimentin. Since vimentin is one of the most abundant proteins within fibroblasts, it is possible that vimentin IFs are major, and perhaps even the major, cargo for dynein. Vimentin IFs also associate with kinesin in vivo, and therefore, the interactions between vimentin and both of these MT-based motors can explain the majority of the bidirectional movements of the various structural forms of vimentin throughout the cell. Furthermore, the interactions of vimentin with the major MT motor proteins also provide important insights into the mechanisms responsible for the long recognized structural relationships observed between MTs and IFs (Goldman, 1971). The observations that IF proteins can be rapidly transported along MTs demonstrate that there are mechanisms that allow for the timely delivery of precursors and the subsequent formation of long IFs within specific areas of the cell (Prahlad et al., 1998). This provides a mechanism for locally controlling the mechanical or structural properties of specific regions of the cytoplasm and establishing the molecular cross talk among the different major cytoskeletal systems. A consequence of abnormal changes in the balance among vimentin, dynein, or kinesin could lead to the accumulation of IF proteins seen in many disease states. These include vimentin aggregates in giant axonal neuropathy (Pena, 1982) and neurofilament aggregates in motor neuron diseases such as Amyotrophic Lateral Sclerosis and Parkinson's Disease (for review see Julien and Mushynski, 1998).

Materials and methods

Cell culture

BHK-21 cells were grown as described (Prahlad et al., 1998). For studies involving the observation of IF particles and squiggles, cells were trypsinized and replated on glass coverslips (Prahlad et al., 1998). In some experiments, 1 μm nocodazole was added to the BHK-21 culture medium. NIH 3T3 cells were grown in DME containing 10% calf serum and antibiotics.

Transfection

Cells were transfected by electroporation and grown in 60-mm dishes according to a previously established protocol (Yoon et al., 2001). At 24–48 h after transfection, cells were trypsinized and replated onto coverslips for immunofluorescence or 100-mm dishes for biochemical analyses (see below). For studies involving immunofluorescence or biochemistry at 6–24 h after transfection, cells were plated onto coverslips or 100-mm culture dishes immediately after electroporation.

GFP-vimentin cDNA was used for transfection to observe vimentin in live cells as described previously (Yoon et al., 1998). Cloning of the p50 (dynamitin) component of dynactin has been described by Echeverri et al. (1996). The p50 insert was excised using NcoI and NotI restriction enzymes and subcloned into a pCMV-Myc expression vector (CLONTECH Laboratories, Inc.).

Antibodies

Polyclonal antibodies directed against BHK-21 vimentin (Yang et al., 1985), bovine brain tubulin, 5H1 (Wang et al., 1993; a gift of Dr. Lester Binder, Northwestern University School of Medicine), and yeast α-tubulin (Serotec, Co.) and a monoclonal antibody against human vimentin (V9; Sigma-Aldrich) were used.

Other antibodies included monoclonal antibodies directed against IC (Chemicon), p50 (dynamitin; BD Biosciences), $p150^{Glued}$ (BD Biosciences), and conventional kinesin (Chemicon). Polyclonal antibodies against LIC1 and 2 (Tynan et al., 2000a), LIC2 (Tynan et al., 2000a), Arp1 (a gift of Dr. David Meyer, University of California, Los Angeles, Los Angeles, CA) (Garces et al., 1999), and the stalk domain (amino acids 523–775) of con-

ventional kinesin (a gift of Dr. Ron Vale, University of California, San Francisco, San Francisco, CA) (Prahlad et al., 1998) were also employed. In addition, a polyclonal antibody directed against amino acids 1776–2242 of the rat cytoplasmic dynein 1 HC was used. Preparation and characterization of this antibody will be described in more detail elsewhere (unpublished data; Tynan et al., 2000b). Monoclonal (Evan et al., 1985) and polyclonal anti–c-myc (Covance) were used to locate cells expressing myc-tagged dynamitin.

FITC-, lissamine-rhodamine–, and Cy5-conjugated anti–mouse, anti–rabbit, and anti–rat antibodies (Jackson ImmunoResearch Laboratories) were used for indirect immunofluorescence. Peroxidase-conjugated anti–rabbit and anti–mouse IgG (Jackson ImmunoResearch Laboratories) were used for immunoblotting. For EM, 18 nm gold particle-conjugated anti–rabbit IgG (Jackson Immunoresearch Laboratories) and 10 nm gold particle-conjugated anti–mouse IgG (Sigma-Aldrich) were used.

Image acquisition and analysis

BHK-21 cells were transfected by electroporation (see above) with GFP-vimentin cDNA 48 h before analysis. In some experiments, cells transfected with GFP-vimentin for 24 h were again transfected with either a vector encoding myc-dynamitin or, as a control, with the pCMV-myc vector without an insert. 24 h after the second transfection, cells were trypsinized and plated onto coverslips to achieve ~70% confluence in standard culture medium (see above) containing 10 mM Hepes, pH 7.0 (Yoon et al., 1998). Live cell observations were made 48–72 h after the first transfection.

Images of cells were acquired with a ZEISS LSM 510 confocal microscope equipped with a 100×, 1.4 NA oil immersion objective (ZEISS). GFP-vimentin was visualized using excitation at 488 nm and emission at 515–545 nm. Images of live cells were acquired from the same focal plane at 5–10-s intervals for 5–10-min periods as described previously (Yoon et al., 1998). Image analysis was performed using the ZEISS LSM 510 software. Rates of movement were calculated using the measure distance function on successive frames as described previously (Yoon et al., 1998). Phase–contrast images were taken simultaneously to ensure that no significant changes in cell shape occurred during observation periods (Yoon et al., 1998).

Indirect immunofluorescence

Cells on coverslips were rinsed with PBS and fixed in either 3.7% formaldehyde (Sigma-Aldrich)/PBS or in methanol (−20°C) for 5 min. After formaldehyde fixation, cells were permeabilized with two 3-min washes in 0.1% NP-40/PBS. After methanol fixation, cells were washed twice in PBS. Subsequently, cells fixed by either method were incubated with a mixture of one to three different primary antibodies for 45 min at 37°C. Cells were then washed with PBS and incubated with secondary antibodies for 30 min. In some experiments, AlexaFluor 568 phalloidin (Molecular Probes) was used to visualize F-actin in formaldehyde-fixed cells. The coverslips were mounted on slides using Gelvatol (Air Products and Chemicals) containing DABCO (Sigma-Aldrich) at 100 mg/ml (Yoon et al., 1998). These preparations were observed in a ZEISS LSM 510 confocal microscope (ZEISS).

In some experiments, cells were treated for 2 min (RT) with different extraction solutions, formaldehyde fixed, and then processed for immunofluorescence as described above. The extraction solutions contained 0.1 M Hepes, pH 7.4, 60 mM Pipes, protease inhibitors (1 mM PMSF and Complete-EDTA free protease inhibitors, 1 tablet/10 ml buffer [Boehringer]) and different concentrations of NaCl (0.1–1 M). In addition, different concentrations (0.1–1.0%) of either digitonin, NP-40, or Triton X-100 were added. Intact IFs were isolated using a modification of a procedure originally described by Starger and Goldman (1977). Briefly, IF-enriched cytoskeletons were prepared by first lysing cells in IF extraction buffer containing 0.5 M NaCl, 100 mM Hepes, pH 7.4, 60 mM Pipes, 1.0% Triton X-100, and Complete-EDTA free protease inhibitors, 1 tablet/10 ml buffer. After 5 min, cells were collected and homogenized, and DNase1 (1 mg/ml) was then added to the solution. IF-enriched cytoskeletons were then pelleted by centrifugation (3,210 *g*; Beckman Allegra 5R centrifuge) and washed three times with the IF extraction buffer.

Platinum replica EM

Ultrastructural observations of cytoskeletal preparations were performed as described elsewhere (Svitkina et al., 1995). For preservation of MTs and IFs, cells on coverslips were extracted with PEM buffer (100 mM Pipes, pH 6.9, 1 mM $MgCl_2$, 1 mM EGTA) containing 1% Triton X-100, 4% PEG, 1 mg/ml DNase 1 (Sigma-Aldrich), and 10 μg/ml Taxol (Sigma-Aldrich) for 5 min (RT). For MT-free IF-enriched cytoskeletal preparations, cells were extracted in PEM buffer with 1% Triton X-100, 0.4 M NaCl, and 1 mg/ml DNase 1 for 10 min. To remove any residual actin, all preparations were treated with recombinant gelsolin NH_2-terminal domain (a gift of Dr. Gary Borisy, Northwestern University School of Medicine) (Verkhovsky and Borisy, 1993). Cells were then fixed with 2% glutaraldehyde and stained with 0.1% tannic acid and 0.2% uranyl acetate. These preparations were then processed by critical point drying followed by rotary shadowing with platinum and carbon (Svitkina et al., 1995). Replicas were removed from the coverslips and transferred to copper grids as described (Svitkina et al., 1995). Immunostaining with primary and secondary gold-coupled antibodies was performed after glutaraldehyde fixation as described (Svitkina et al., 1995). Controls for these preparations involved all of the various steps and incubations described above using either no antibodies or secondary gold-coupled antibodies alone.

SDS-PAGE and immunoblotting

For biochemical studies, BHK-21 cells were grown on 150-mm dishes to 60% confluency, washed twice with PBS, and IF-enriched cytoskeletons were prepared (see above). These cytoskeletons were sonicated in Laemmli buffer containing 1% β-mercaptoethanol and boiled for 5 min (Laemmli, 1970). The samples were separated on 7.5 or 10% polyacrylamide gels according to the method of Laemmli (1970). Immunoblotting was performed according to Towbin et al. (1979). Primary and secondary antibodies used for immunoblotting were described above. Some immunoblots were developed by ECL (Amersham Pharmacia Biotech).

The authors thank Dr. Tatyana Svitkina and Ms. Kyung-Hee Myung for their help with EM. We also want to thank Dr. David Meyer for sending us the Arp1 antibody. We greatly appreciate the assistance of the entire Goldman lab during the preparation of this article. We wish to note that this paper was revised and submitted 48 h prior to the marriage of Brian to Marni and we wish to express our appreciation to the bride-to-be.

This work has been supported by Method to Extend Research in Time Awards from the National Institutes of General Medical Sciences to R.D. Goldman (GM 36806) and R.B. Vallee (GM 47434), and a grant from the National Institute of Alcohol Abuse and Alcoholism to B.T. Helfand (F30-AA13470-01).

Submitted: 7 February 2002
Revised: 5 April 2002
Accepted: 24 April 2002

References

Avsyuk, A., A.A. Minin, and F.K. Gyoeva. 1995. Kinesin associated with vimentin intermediate filaments contains a specific light chain. *Dokl. Biol. Sci.* 345: 644–646.

Burkhardt, J.K., C.J. Echeverri, T. Nilsson, and R.B. Vallee. 1997. Overexpression of the dynamitin (p50) subunit of the dynactin complex disrupts dynein-dependent maintenance of membrane organelle distribution. *J. Cell Biol.* 139:469–484.

Chou, Y.H., B.T. Helfand, and R.D. Goldman. 2001. New horizons in cytoskeletal dynamics: transport of intermediate filaments along microtubule tracks. *Curr. Opin. Cell Biol.* 13:106–109.

Durham, H.D., S.D. Pena, and S. Carpenter. 1983. The neurotoxins 2,5-hexanedione and acrylamide promote aggregation of intermediate filaments in cultured fibroblasts. *Muscle Nerve.* 6:631–637.

Echeverri, C.J., B.M. Paschal, K.T. Vaughan, and R.B. Vallee. 1996. Molecular characterization of the 50-kD subunit of dynactin reveals function for the complex in chromosome alignment and spindle organization during mitosis. *J. Cell Biol.* 132:617–633.

Evan, G.I., G.K. Lewis, G. Ramsay, and J.M. Bishop. 1985. Isolation of monoclonal antibodies specific for human c-myc proto-oncogene product. *Mol. Cell. Biol.* 5:3610–3616.

Gao, Y., and E. Sztul. 2001. A novel interaction of the Golgi complex with the vimentin intermediate filament cytoskeleton. *J. Cell Biol.* 152:877–894.

Garces, J.A., I.B. Clark, D.I. Meyer, and R.B. Vallee. 1999. Interaction of the p62 subunit of dynactin with Arp1 and the cortical actin cytoskeleton. *Curr. Biol.* 9:1497–1500.

Goldman, R.D. 1971. The role of three cytoplasmic fibers in BHK-21 cell motility. I. Microtubules and the effects of colchicine. *J. Cell Biol.* 51:752–762.

Gyoeva, F.K., and V.I. Gelfand. 1991. Coalignment of vimentin intermediate filaments with microtubules depends on kinesin. *Nature.* 353:445–448.

Heath, C.M., M. Windsor, and T. Wileman. 2001. Aggresomes resemble sites specialized for virus assembly. *J. Cell Biol.* 153:449–455.

Holleran, E.A., M.K. Tokito, S. Karki, and E.L. Holzbaur. 1996. Centractin

(ARP1) associates with spectrin revealing a potential mechanism to link dynactin to intracellular organelles. *J. Cell Biol.* 135:1815–1829.

Holleran, E.A., L.A. Ligon, M. Tokito, M.C. Stankewich, J.S. Morrow, and E.L. Holzbaur. 2001. beta III spectrin binds to the Arp1 subunit of dynactin. *J. Biol. Chem.* 276:36598–36605.

Howell, B.J., B.F. McEwen, J.C. Canman, D.B. Hoffman, E.M. Farrar, C.L. Rieder, and E.D. Salmon. 2001. Cytoplasmic dynein/dynactin drives kinetochore protein transport to the spindle poles and has a role in mitotic spindle checkpoint inactivation. *J. Cell Biol.* 155:1159–1172.

Julien, J.P., and W.E. Mushynski. 1998. Neurofilaments in health and disease. *Prog. Nucleic Acid Res. Mol. Biol.* 61:1–23.

Karki, S., and E.L. Holzbaur. 1995. Affinity chromatography demonstrates a direct binding between cytoplasmic dynein and the dynactin complex. *J. Biol. Chem.* 270:28806–28811.

King, S.J., and T.A. Schroer. 2000. Dynactin increases the processivity of the cytoplasmic dynein motor. *Nat. Cell Biol.* 2:20–24.

Kreitzer, G., G. Liao, and G.G. Gundersen. 1999. Detyrosination of tubulin regulates the interaction of intermediate filaments with microtubules in vivo via a kinesin-dependent mechanism. *Mol. Biol. Cell.* 10:1105–1118.

Laemmli, U.K. 1970. Cleavage of structural proteins during the assembly of the head of bacteriophage T4. *Nature.* 227:680–685.

Lamb, N.J., A. Fernandez, J.R. Feramisco, and W.J. Welch. 1989. Modulation of vimentin containing intermediate filament distribution and phosphorylation in living fibroblasts by the cAMP-dependent protein kinase. *J. Cell Biol.* 108:2409–2422.

Liao, G., and G.G. Gundersen. 1998. Kinesin is a candidate for cross-bridging microtubules and intermediate filaments. Selective binding of kinesin to detyrosinated tubulin and vimentin. *J. Biol. Chem.* 273:9797–9803.

Navone, F., J. Niclas, N. Hom-Booher, L. Sparks, H.D. Bernstein, G. McCaffrey, and R.D. Vale. 1992. Cloning and expression of a human kinesin heavy chain gene: interaction of the COOH-terminal domain with cytoplasmic microtubules in transfected CV-1 cells. *J. Cell Biol.* 117:1263–1275.

Noda, Y., Y. Okada, N. Saito, M. Setou, Y. Xu, Z. Zhang, and N. Hirokawa. 2001. KIFC3, a microtubule minus end–directed motor for the apical transport of annexin XIIIb-associated Triton-insoluble membranes. *J. Cell Biol.* 155:77–88.

Osborn, M., W. Franke, and K. Weber. 1980. Direct demonstration of the presence of two immunologically distinct intermediate-sized filament systems in the same cell by double label immunofluorescence microscopy. Vimentin and cytokeratin fibers in cultured epithelial cells. *Exp. Cell Res.* 125:37–46.

Pena, S.D. 1982. Giant axonal neuropathy: an inborn error of organization of intermediate filaments. *Muscle Nerve.* 5:166–172.

Prahlad, V., M. Yoon, R.D. Moir, R.D. Vale, and R.D. Goldman. 1998. Rapid movements of vimentin on microtubule tracks: kinesin-dependent assembly of intermediate filament networks. *J. Cell Biol.* 143:159–170.

Prahlad, V., B.T. Helfand, G.M. Langford, R.D. Vale, and R.D. Goldman. 2000. Fast transport of neurofilament protein along microtubules in squid axoplasm. *J. Cell Sci.* 113:3939–3946.

Presley, J.F., N.B. Cole, T.A. Schroer, K. Hirschberg, K.J. Zaal, and J. Lippincott-Schwartz. 1997. ER-to-Golgi transport visualized in living cells. *Nature.* 389:81–85.

Purohit, A., S.H. Tynan, R. Vallee, and S.J. Doxsey. 1999. Direct interaction of pericentrin with cytoplasmic dynein light intermediate chain contributes to mitotic spindle organization. *J. Cell Biol.* 147:481–492.

Quintyne, N.J., S.R. Gill, D.M. Eckley, C.L. Crego, D.A. Compton, and T.A. Schroer. 1999. Dynactin is required for microtubule anchoring at centrosomes. *J. Cell Biol.* 147:321–334.

Rogalski, A.A., and S.J. Singer. 1984. Associations of elements of the Golgi apparatus with microtubules. *J. Cell Biol.* 99:1092–1100.

Roghi, C., and V.J. Allan. 1999. Dynamic association of cytoplasmic dynein heavy chain 1a with the Golgi apparatus and intermediate compartment. *J. Cell Sci.* 112:4673–4685.

Roy, S., P. Coffee, G. Smith, R.K. Liem, S.T. Brady, and M.M. Black. 2000. Neurofilaments are transported rapidly but intermittently in axons: implications for slow axonal transport. *J. Neurosci.* 20:6849–6861.

Shah, J.V., L.A. Flanagan, P.A. Janmey, and J.F. Leterrier. 2000. Bidirectional translocation of neurofilaments along microtubules mediated in part by dynein/dynactin. *Mol. Biol. Cell.* 11:3495–3508.

Sharp, D.J., G.C. Rogers, and J.M. Scholey. 2000. Cytoplasmic dynein is required for poleward chromosome movement during mitosis in *Drosophila* embryos. *Nat. Cell Biol.* 2:922–930.

Starger, J.M., and R.D. Goldman. 1977. Isolation and preliminary characterization of 10-nm filaments from baby hamster kidney (BHK-21) cells. *Proc. Natl. Acad. Sci. USA.* 74:2422–2426.

Starr, D.A., B.C. Williams, T.S. Hays, and M.L. Goldberg. 1998. ZW10 helps recruit dynactin and dynein to the kinetochore. *J. Cell Biol.* 142:763–774.

Straube-West, K., P.A. Loomis, P. Opal, and R.D. Goldman. 1996. Alterations in neural intermediate filament organization: functional implications and the induction of pathological changes related to motor neuron disease. *J. Cell Sci.* 109:2319–2329.

Suomalainen, M., M.Y. Nakano, S. Keller, K. Boucke, R.P. Stidwill, and U.F. Greber. 1999. Microtubule-dependent plus- and minus end–directed motilities are competing processes for nuclear targeting of adenovirus. *J. Cell Biol.* 144:657–672.

Svitkina, T.M., A.B. Verkhovsky, and G.G. Borisy. 1995. Improved procedures for electron microscopic visualization of the cytoskeleton of cultured cells. *J. Struct. Biol.* 115:290–303.

Tai, A.W., J.Z. Chuang, C. Bode, U. Wolfrum, and C.H. Sung. 1999. Rhodopsin's carboxy-terminal cytoplasmic tail acts as a membrane receptor for cytoplasmic dynein by binding to the dynein light chain Tctex-1. *Cell.* 97:877–887.

Tai, C.Y., D.L. Dujardin, N.E. Faulkner, and R.B. Vallee. 2002. Role of dynein, dynactin, and CLIP-170 interactions in LIS1 kinetochore function. *J Cell Biol.* 156:959–968.

Towbin, H., T. Staehelin, and J. Gordon. 1979. Electrophoretic transfer of proteins from polyacrylamide gels to nitrocellulose sheets: procedure and some applications. *Proc. Natl. Acad. Sci. USA.* 76:4350–4354.

Tynan, S.H., M.A. Gee, and R.B. Vallee. 2000a. Distinct but overlapping sites within the cytoplasmic dynein heavy chain for dimerization and for intermediate chain and light intermediate chain binding. *J. Biol. Chem.* 275:32769–32774.

Tynan, S.H., A. Purohit, S.J. Doxsey, and R.B. Vallee. 2000b. Light intermediate chain 1 defines a functional subfraction of cytoplasmic dynein which binds to pericentrin. *J. Biol. Chem.* 275:32763–32768.

Vallee, R.B., and M.P. Sheetz. 1996. Targeting of motor proteins. *Science.* 271: 1539–1544.

Vaughan, K.T., and R.B. Vallee. 1995. Cytoplasmic dynein binds dynactin through a direct interaction between the intermediate chains and p150Glued. *J. Cell Biol.* 131:1507–1516.

Verkhovsky, A.B., and G.G. Borisy. 1993. Nonsarcomeric mode of myosin II organization in the fibroblast lamellum. *J. Cell Biol.* 123:637–652.

Wang, Y., P.A. Loomis, R.P. Zinkowski, and L.I. Binder. 1993. A novel tau transcript in cultured human neuroblastoma cells expressing nuclear tau. *J. Cell Biol.* 121:257–267.

Wang, L., C.L. Ho, D. Sun, R.K. Liem, and A. Brown. 2000. Rapid movement of axonal neurofilaments interrupted by prolonged pauses. *Nat. Cell Biol.* 2:137–141.

Welch, W.J., and J.P. Suhan. 1985. Morphological study of the mammalian stress response: characterization of changes in cytoplasmic organelles, cytoskeleton, and nucleoli, and appearance of intranuclear actin filaments in rat fibroblasts after heat-shock treatment. *J. Cell Biol.* 101:1198–1211.

Yabe, J.T., A. Pimenta, and T.B. Shea. 1999. Kinesin-mediated transport of neurofilament protein oligomers in growing axons. *J. Cell Sci.* 112:3799–3814.

Yang, H.Y., N. Lieska, A.E. Goldman, and R.D. Goldman. 1985. A 300,000-mol-wt intermediate filament-associated protein in baby hamster kidney (BHK-21) cells. *J. Cell Biol.* 100:620–631.

Yano, H., F.S. Lee, H. Kong, J. Chuang, J. Arevalo, P. Perez, C. Sung, and M.V. Chao. 2001. Association of Trk neurotrophin receptors with components of the cytoplasmic dynein motor. *J. Neurosci.* 21:RC125.

Yoon, K.H., M. Yoon, R.D. Moir, S. Khuon, and R.D. Goldman. 2001. The motility and assembly of keratin tonofibrils in living epithelial cells. *J. Cell Biol.* 153:503–516.

Yoon, M., R.D. Moir, V. Prahlad, and R.D. Goldman. 1998. Motile properties of vimentin intermediate filament networks in living cells. *J. Cell Biol.* 143:147–157.

Young, A., J.B. Dictenberg, A. Purohit, R. Tuft, and S.J. Doxsey. 2000. Cytoplasmic dynein-mediated assembly of pericentrin and gamma tubulin onto centrosomes. *Mol. Biol. Cell.* 11:2047–2056.